



Project ID: mat153

A Multi-Scale Computational Platform for Predictive Modeling of Corrosion in Al-Steel Joints

PI: S. J. Hu (2019), M. Banu (2019-2021)

Presenter: M. Banu

The University of Michigan

June 3, 2020

This presentation does not contain any proprietary, confidential, or otherwise restricted information.

Project ID: mat153

Overview

Timeline

- Project start: **1/01/2019**
- Project end: **12/31/2021**
- Percent complete: **45%**

Budget

- Total project funding
 - DOE share: **\$1,500,000**
 - Contractor share: **\$478,431**

Barriers and Technical Targets

- Multi-material systems
- Aluminum – Steel joints
- Corrosion
- Develop predictive models for dissimilar Al-Steel joints (within 10% of experiments) to enable mixed material structures

"USDRIVE Materials Technical Team Roadmap October 2017, section 6"

Partners

- Pennsylvania State University (Penn State)
- University of Illinois (Illinois)
- University of Georgia (UGa)
- General Motors Company (GM)
- Optimal Process Technologies (OPT)
- LST, an ANSYS Company (LS-Dyna)

Project lead: University of Michigan (UM)

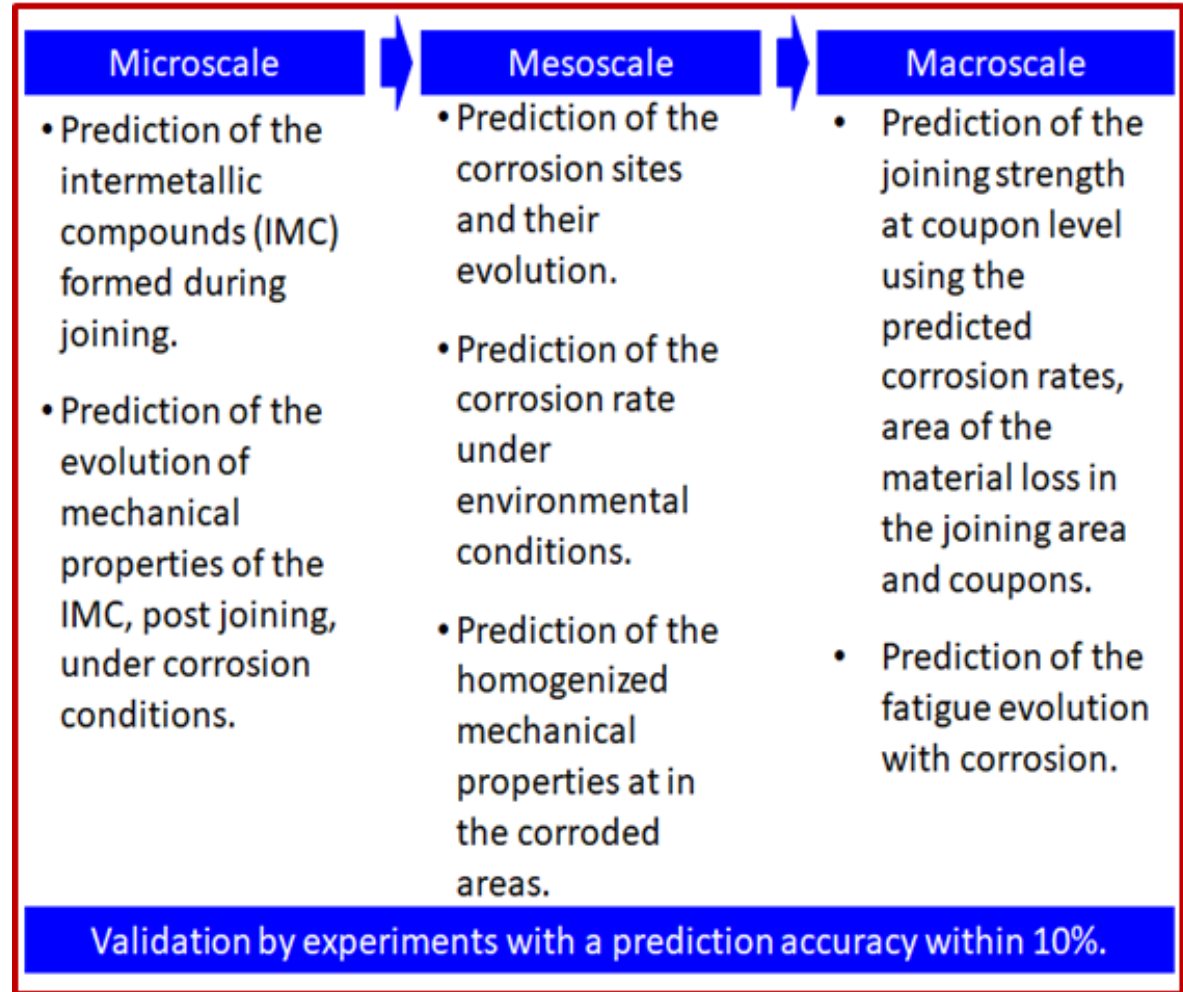
Project Objective

- To develop and validate a multi-scale model to predict the location and extent of corrosion in Al-steel joints and the impact of such corrosion on joint strength and fatigue life.

Relevance

- The global cost of corrosion was estimated at about 3.4% of the global GDP in 2013. By using available corrosion control practices, it is estimated a saving between 15-35% of the cost of corrosion.
- Corrosion in transportation has many serious economic, health, safety, technological consequences.
- Prediction of the corrosion and its impact on performance of the dissimilar material joints is critical for reducing the massive number of the current corrosion-based recalls.
- Such models enable extensive use of the other multi-material systems for light-weighting.

Multi-scale model to predict the location and extent of corrosion in dissimilar joints



Milestones

2020

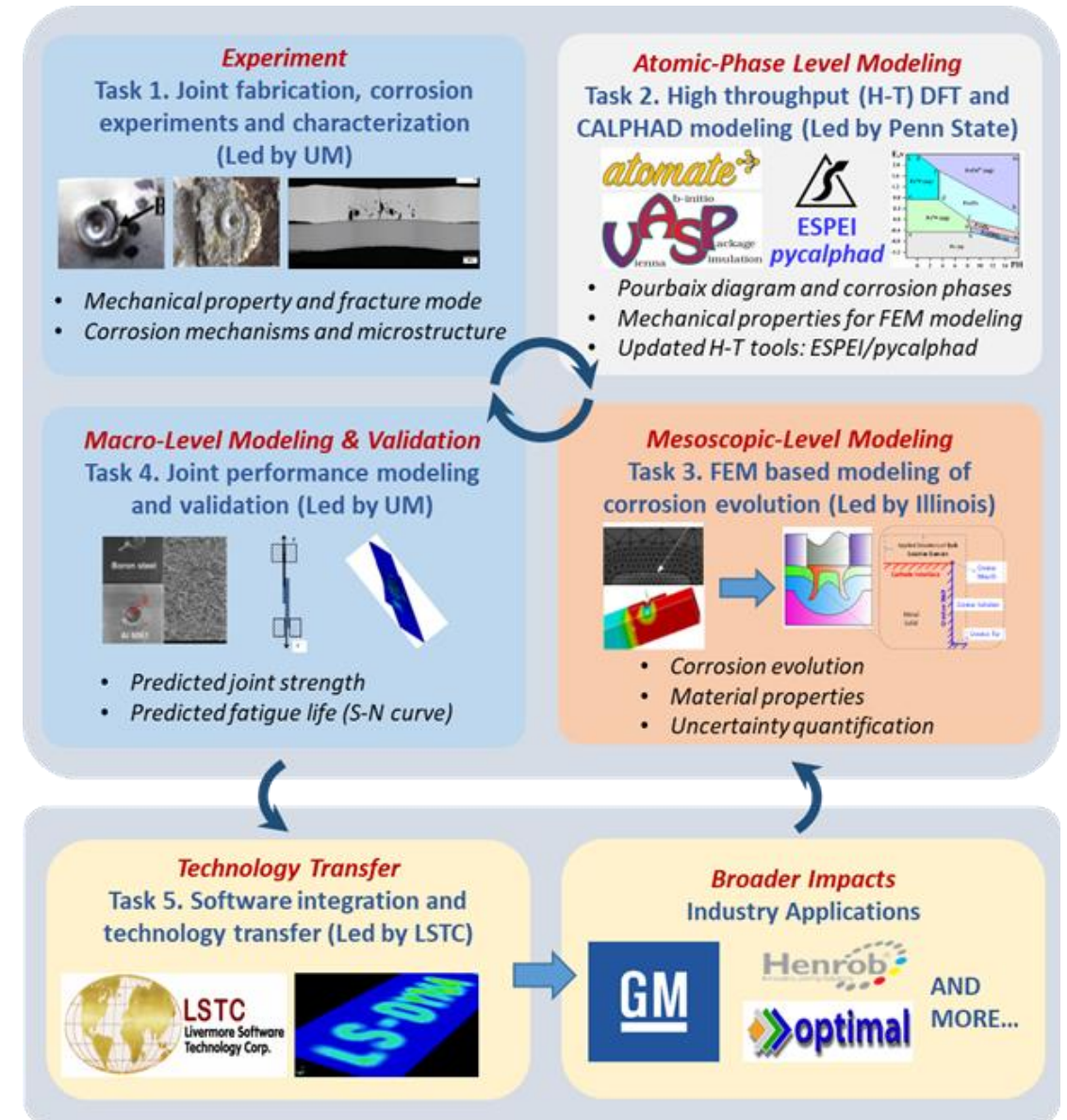
Date	Milestones and Go/No Go Decisions	Status
(March-30)	<u>Technical milestone</u> Material Property Parameters	100%
(June-30)	<u>Technical milestone</u> Material Property CALPHAD Databases	On track
(Sept.-30)	<u>Technical milestone</u> Joint Performance Prediction	On track
(Dec.-20)	<u>Technical milestone</u> LS-Dyna Platform Module of Material and Joint Performance	On track
(Dec.-20)	Go/No Go Decision Extended model of corrosion evolution	On track

2021

Date	Milestones and Go/No Go Decisions	Status
(June-30)	<u>Technical milestone</u> Corrosion Evolution Model Verification	On track
(March-30)	<u>Technical milestone</u> Multiscale Simulation Model Integration	On track
(Sept.-30)	<u>Technical milestone</u> Uncertainty Quantification Model Integration	On track
(Sept.-30)	<u>Technical milestone</u> Fatigue Performance Prediction	On track
(Dec.-20)	Go/No Go Decision Force-Displacement Prediction	On track

Approach / Strategy

1. Atomic-phase Level modeling with high throughput DFT and CALPHAD
2. Mesoscopic modeling with integrated uncertainty quantification
3. Macro-scale modeling for joint performance prediction
4. Dissimilar material joining and corrosion testing
5. Software integration

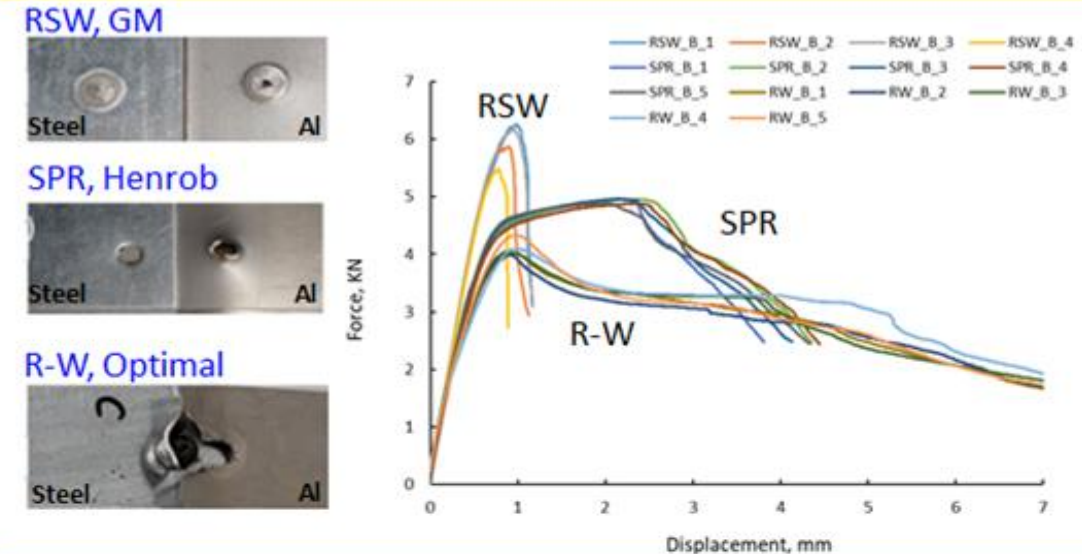


Accomplishment

- Identified a robust process window for joining a lap shear configuration of HSLA 340 2.0mm and aluminum A6022, 1.2 mm using RSW at GM, SPR at Henrob and rivet-welding R-W at Optimal. RSW - 900lb force, 3 welding stages, 250 ms holding time. SPR and R-W - 5 mm rivet, Zn-carbon steel coated, 315mm/s.
- Determined the reference welding performance of each technology before corrosion (UM & GM) using lap share tests with a speed of 2 mm/min. Force displacement curves were plotted for the three technologies. Between 4-5 replicates were used for each technology.
- Accelerated corrosion tests that matches the form and degree of corrosion in vehicle application environments in 1cyle, 7 cycles, 14 cycles, 26 cycles, 48 cycles, 72 cycles, 104 cycles (standard GM14872, GM & UM).

Lap shear joining performance after corrosion shows a similar evolution for RSW and SPR characterized by a 2% increase in the maximum force from 1 to 48 cycle followed by a drop of the force for the rest of the cycles.

Lap shear joining performance before corrosion



Accelerated corrosion tests

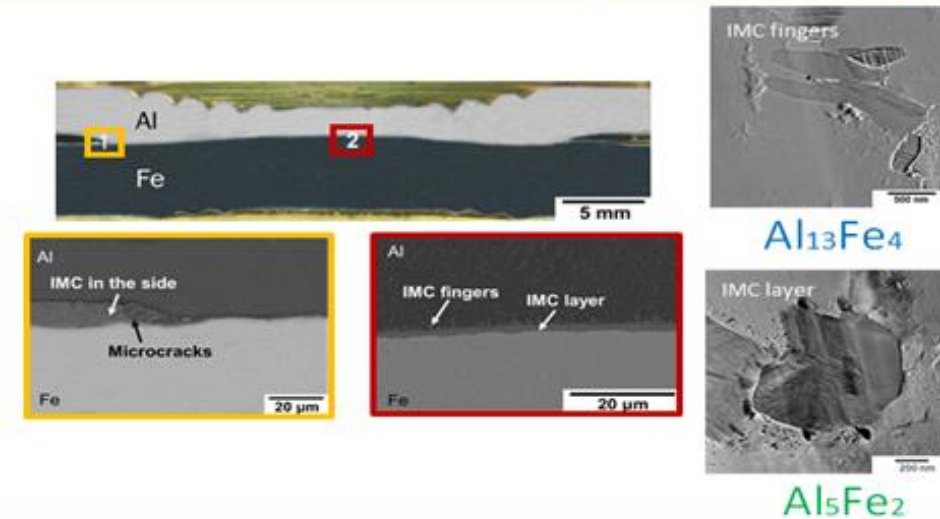


Accomplishment

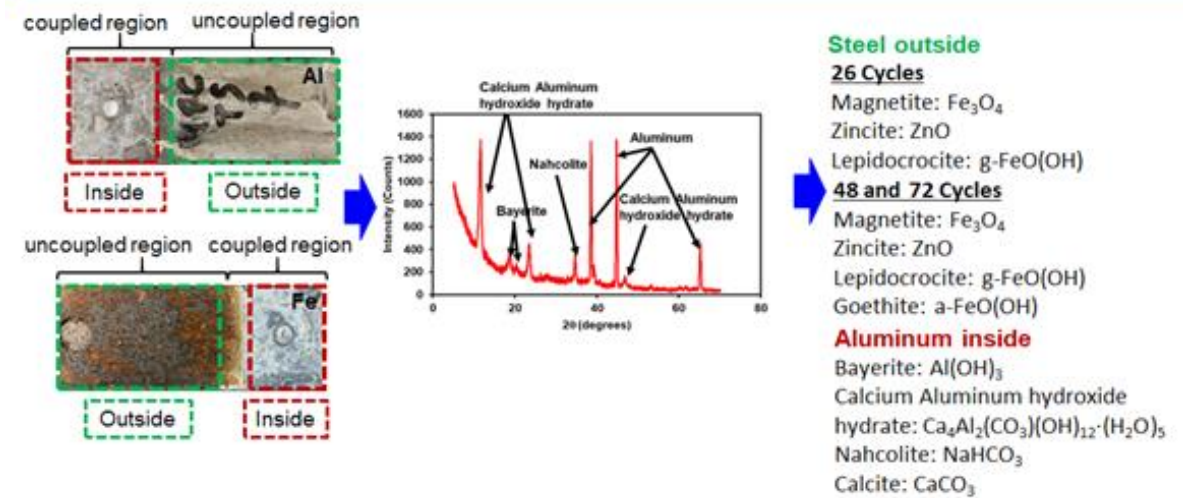
- Identified bonding interfacial characteristics in corroded samples and compare with no-corroded.
- Determined the common corrosion products developed in RSW and SPR (experimental).
- Determined the volume fraction for each intermetallic compound.
- Created a material databased for validation of the predicted intermetallic compounds.
- Characterized RSW and SPR joining interfaces.
- R-W is a coupled RSW and SPR process, hence models will be developed based on RSW and SPR and verified on R-W.

Three layers are seen at IMC in the middle of the interface, which consist of two layers of Al_5Fe_2 , and finger-like $\text{Al}_{13}\text{Fe}_4$. A clear grain boundary is observed between the two Al_5Fe_2 layers, indicating different grain orientations. Some $\text{Al}_8\text{Fe}_2\text{Si}$ particles are also seen.

RSW before corrosion (SEM and TEM)



RSW after 26, 48 and 72 corrosion cycles

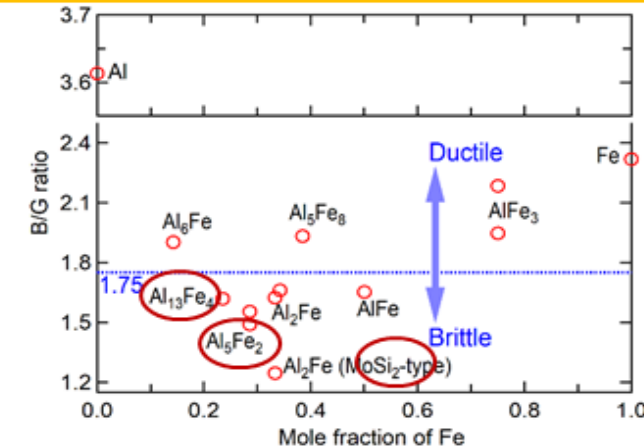


Accomplishment

- DFT calculations and machine learning (ML) predictions of thermodynamic, corrosion and mechanical properties; CALPHAD modeling to predict properties of individual phases (Task 2.1-2.2).
- Machine learning (ML) predictions, DFT-based first-principles calculations, and high throughput CALPHAD modeling (Tasks 2.1-2.3)
- Phase diagram and Pourbaix corrosion diagram as a function of composition, temperature, pressure, electrochemical potential, and pH value (Task 2.3).
- Predictions of mechanical properties: elastic properties, critical resolved shear stress, ideal shear strength, and stress-strain curves (Tasks 2.1 and 2.4).

Prediction of $\text{Al}_{13}\text{Fe}_4$ and Al_2Fe_5 phases is validated by the experiments. In corrosion conditions, their behavior is changing from ductile to brittle.

Predicted Al-Fe IMCs during welding conditions



By considering thermodynamic and kinetic affects (high temperatures, high pressures, and fast cooling)

By considering thermodynamic and kinetic affects:

- Al_2Fe_5 is the most possible IMCs to be formed at high T (> 930 K, with the existence of liquid phase), followed by $\text{Al}_{13}\text{Fe}_4$ (or Al_3Fe in some references), Al_2Fe is also can be formed if T is high
- Al_6Fe is a pressure-favorable IMC, stable at low T
- At low temperatures (e.g., < 930 K), Al-rich IMCs will form, $\text{Al}_{13}\text{Fe}_4$ and also Al_6Fe (Al_6Fe is a pressure-favorable IMC, stable at low T)

Accomplishment

- Two case studies were carried out for understanding and predicting the formation of Al-Fe IMCs during welding conditions and formation of IMCs of Al-Fe joins in corrosion conditions.
- The Material Property CALPHAD Database contains:
 - List of IMCs for RSW and SPR.
 - List of corrosion products at different corrosion cycles.
 - Thermodynamic properties of Al-Fe IMCs as a function of temperature and pressure and thermodynamic properties of Al-Fe-based corrosion products at 0K.
 - Mechanical database, i.e. elastic properties of Al-Fe IMCs and their impact on material behavior change.

IMCs elastic properties are important for modeling the joining constitutive material behavior.

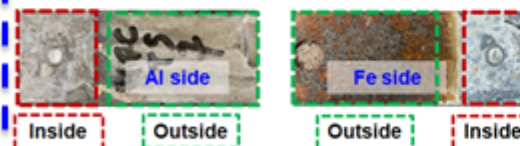
Evolution of the properties with corrosion are important for modeling and prediction of damage in joining.

Material Property CALPHAD DATABASE

RSW: Corrosion products					SPR: Corrosion products				
Cycles	Al Inside	Al Outside	Fe Inside	Fe Outside	Cycles	Al Inside	Al Outside	Fe Inside	Fe Outside
1	Al	$\text{Al}(\text{OH})_3$ $\text{Ca}_4\text{Al}_2(\text{CO}_3)(\text{OH})_{12}$ (H_2O) ₅	Zn	$\text{Zn}(\text{OH})_2\text{Cl}_2(\text{H}_2\text{O})$ Zn	1	Uncorroded	Al	$\text{Zn}_9(\text{OH})_8\text{Cl}_2(\text{H}_2\text{O})$ $\text{Zn}_9(\text{CO}_3)_2(\text{OH})_8$ $\text{Zn}_9(\text{OH})_8\text{Cl}_2(\text{H}_2\text{O})$ Zn	ZnO
7	$\text{Al}(\text{OH})_3$ $\text{Ca}_4\text{Al}_2(\text{CO}_3)(\text{OH})_{12}$ (H_2O) ₅	$\text{Al}(\text{OH})_3$ $\text{Ca}_4\text{Al}_2(\text{CO}_3)(\text{OH})_{12}$ (H_2O) ₅	$\text{Fe}(\text{OH})_{12}(\text{CO}_3)$ ZnO $\text{Zn}_9(\text{CO}_3)_2(\text{OH})_8$ $\text{Zn}_9(\text{OH})_8\text{Cl}_2(\text{H}_2\text{O})$	$\text{Fe}(\text{OH})_{12}(\text{CO}_3)$ $\text{Zn}_9(\text{CO}_3)_2(\text{OH})_8$ $\text{Zn}_9(\text{OH})_8\text{Cl}_2(\text{H}_2\text{O})$ ZnO	7	Uncorroded	$\text{Al}(\text{OH})_3$ $\text{Ca}_4\text{Al}_2(\text{CO}_3)(\text{OH})_{12}$ (H_2O) ₅	$\text{Fe}(\text{OH})_{12}(\text{CO}_3)$ ZnO $\text{Zn}_9(\text{CO}_3)_2(\text{OH})_8$ $\text{Zn}_9(\text{OH})_8\text{Cl}_2(\text{H}_2\text{O})$ Zn	$\text{Fe}(\text{OH})_{12}(\text{CO}_3)$ $\text{Zn}_9(\text{CO}_3)_2(\text{OH})_8$ $\text{Zn}_9(\text{OH})_8\text{Cl}_2(\text{H}_2\text{O})$ ZnO
14	$\text{Al}(\text{OH})_3$ $\text{Ca}_4\text{Al}_2(\text{CO}_3)(\text{OH})_{12}$ (H_2O) ₅	$\text{Al}(\text{OH})_3$ $\text{Ca}_4\text{Al}_2(\text{CO}_3)(\text{OH})_{12}$ (H_2O) ₅	$\text{Fe}(\text{OH})_{12}(\text{CO}_3)$ ZnO $\text{Zn}_9(\text{CO}_3)_2(\text{OH})_8$ $\text{Zn}_9(\text{OH})_8\text{Cl}_2(\text{H}_2\text{O})$	$\text{Fe}(\text{OH})_{12}(\text{CO}_3)$ $\text{Zn}_9(\text{CO}_3)_2(\text{OH})_8$ $\text{Zn}_9(\text{OH})_8\text{Cl}_2(\text{H}_2\text{O})$ ZnO	14	Uncorroded	$\text{Al}(\text{OH})_3$ $\text{Ca}_4\text{Al}_2(\text{CO}_3)(\text{OH})_{12}$ (H_2O) ₅	$\text{Fe}(\text{OH})_{12}(\text{CO}_3)$ ZnO $\text{Zn}_9(\text{CO}_3)_2(\text{OH})_8$ $\text{Zn}_9(\text{OH})_8\text{Cl}_2(\text{H}_2\text{O})$ Zn	$\text{Fe}(\text{OH})_{12}(\text{CO}_3)$ $\text{Zn}_9(\text{CO}_3)_2(\text{OH})_8$ $\text{Zn}_9(\text{OH})_8\text{Cl}_2(\text{H}_2\text{O})$ ZnO
26	$\text{Al}(\text{OH})_3$ $\text{Ca}_4\text{Al}_2(\text{CO}_3)(\text{OH})_{12}$ (H_2O) ₅	$\text{Al}(\text{OH})_3$ $\text{Ca}_4\text{Al}_2(\text{CO}_3)(\text{OH})_{12}$ (H_2O) ₅	$\text{Fe}(\text{OH})_{12}(\text{CO}_3)$ ZnO $\text{Zn}_9(\text{CO}_3)_2(\text{OH})_8$ $\text{Zn}_9(\text{OH})_8\text{Cl}_2(\text{H}_2\text{O})$	Fe_3O_4 ZnO $\gamma\text{-FeO}(\text{OH})$	26	Uncorroded	$\text{Al}(\text{OH})_3$ $\text{Ca}_4\text{Al}_2(\text{CO}_3)(\text{OH})_{12}$ (H_2O) ₅	$\text{Fe}(\text{OH})_{12}(\text{CO}_3)$ ZnO $\text{Zn}_9(\text{CO}_3)_2(\text{OH})_8$ $\text{Zn}_9(\text{OH})_8\text{Cl}_2(\text{H}_2\text{O})$ Zn	Fe_3O_4 ZnO $\gamma\text{-FeO}(\text{OH})$
48	$\text{Al}(\text{OH})_3$ $\text{Ca}_4\text{Al}_2(\text{CO}_3)(\text{OH})_{12}$ (H_2O) ₅	$\text{Al}(\text{OH})_3$ $\text{Ca}_4\text{Al}_2(\text{CO}_3)(\text{OH})_{12}$ (H_2O) ₅	$\text{Fe}(\text{OH})_{12}(\text{CO}_3)$ ZnO $\text{Zn}_9(\text{CO}_3)_2(\text{OH})_8$	Fe_3O_4 ZnO $\gamma\text{-FeO}(\text{OH})$ $\alpha\text{-FeO}(\text{OH})$	48	Uncorroded	$\text{Al}(\text{OH})_3$ $\text{Ca}_4\text{Al}_2(\text{CO}_3)(\text{OH})_{12}$ (H_2O) ₅	$\text{Fe}(\text{OH})_{12}(\text{CO}_3)$ ZnO $\text{Zn}_9(\text{CO}_3)_2(\text{OH})_8$	Fe_3O_4 ZnO $\gamma\text{-FeO}(\text{OH})$ $\alpha\text{-FeO}(\text{OH})$
72	$\text{Al}(\text{OH})_3$ $\text{Ca}_4\text{Al}_2(\text{CO}_3)(\text{OH})_{12}$ (H_2O) ₅	$\text{Al}(\text{OH})_3$ CaCO_3	$\text{Fe}(\text{OH})_{12}(\text{CO}_3)$ ZnO $\text{Zn}_9(\text{CO}_3)_2(\text{OH})_8$ Fe_3O_4	Fe_3O_4 ZnO $\gamma\text{-FeO}(\text{OH})$ $\alpha\text{-FeO}(\text{OH})$	72	Uncorroded	$\text{Al}(\text{OH})_3$ $\text{Ca}_4\text{Al}_2(\text{CO}_3)(\text{OH})_{12}$ (H_2O) ₅	$\text{Fe}(\text{OH})_{12}(\text{CO}_3)$ ZnO $\text{Zn}_9(\text{CO}_3)_2(\text{OH})_8$	Fe_3O_4 ZnO $\gamma\text{-FeO}(\text{OH})$ $\alpha\text{-FeO}(\text{OH})$
104	$\text{Al}(\text{OH})_3$ $\text{Ca}_4\text{Al}_2(\text{CO}_3)(\text{OH})_{12}$ (H_2O) ₅	CaCO_3 $\text{Al}(\text{OH})_3$ Al_2O_3	$\text{Fe}(\text{OH})_{12}(\text{CO}_3)$ ZnO Fe_3O_4	Fe_3O_4 ZnO $\gamma\text{-FeO}(\text{OH})$ $\alpha\text{-FeO}(\text{OH})$					

Material database was built. There are 90% common material components in RSW and SPR (colored in green).

Legend for corrosion products



Predicted elastic properties:

B_0 - Bulk Modulus (GPa)
 G_0 - Shear Modulus (GPa)
 Y_0 - Young Modulus (GPa)
 B_0/G_0 (>1.75 for ductile materials)
 Poisson ratio
 A^U - Anisotropic index (0 for isotropic single crystals)

IMCs	B_0 (GPa)	G_0 (GPa)	Y_0 (GPa)	Poisson	B_0/G_0	A^U
Al	77.8	20.9	57.5	0.377	3.73	0.329
	79	29	78	0.34		
Al_2Fe	106.6	53.0	136.4	0.287	2.01	0.694
$\text{Al}_{13}\text{Fe}_4$	125.6	76.7	191.2	0.247	1.64	0.163
Al_3Fe_5	141.8	73.3	187.6	0.279	1.93	0.001
Al_2Fe (MoSi ₂ -type)	154.7	115.8	278.0	0.201	1.34	0.812
Al_2Fe (structure 1)	134.3	79.8	199.8	0.252	1.68	0.147
Al_2Fe (structure 2)	136.9	83.3	207.8	0.247	1.64	0.134
AlFe	184.0	102.5	259.3	0.265	1.79	0.951
Al_3Fe_2 (structure 1)	132.6	87.8	215.8	0.229	1.51	0.177
Al_3Fe_2 (USPEX)	137.0	83.7	208.6	0.247	1.64	0.664
AlFe_3 (structure 1)	188.3	56.5	154.1	0.367	3.33	11.04
AlFe_3 (structure 2)	197.2	81.0	213.7	0.321	2.43	3.343
Fe	180.6	76.5	201.1	0.315	2.36	0.196
	173	87	223	0.29		

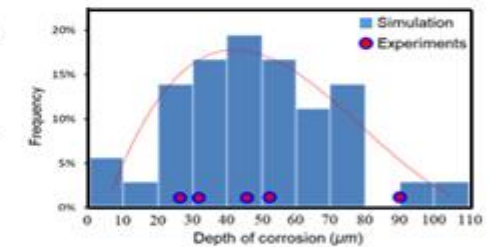
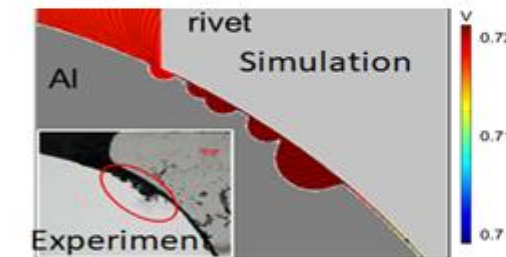
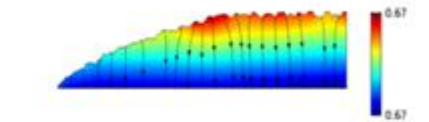
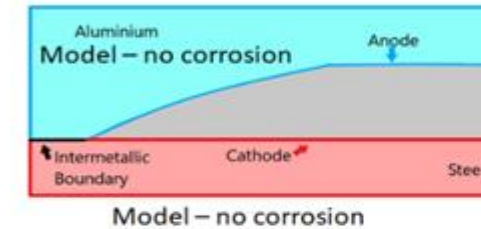
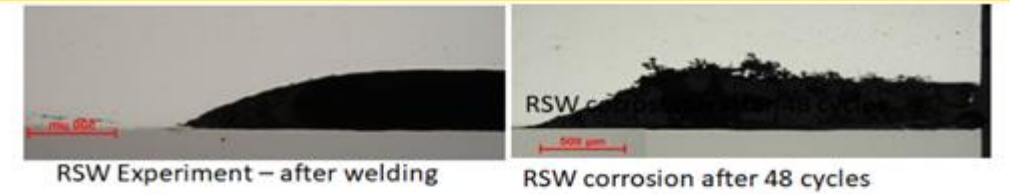
Accomplishment

- Developed finite element based mesoscopic corrosion models, which bridges the atomistic model with the continuum scale models while taking accurate DFT calculations as the model inputs.
- Simulate the evolution of corrosion from the modeling of electrochemical environment in crevices and pits due to galvanic corrosion in aqueous media, considering different conditions such as the coupling with the thermal & stress fields, the geometric parameters as well as the electrode/electrolyte compositions and the uncertainties.
- Developed corrosion models serve as the material behavior inputs for joint performance predictions using continuum scale models.

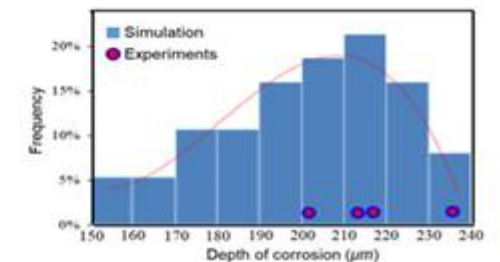
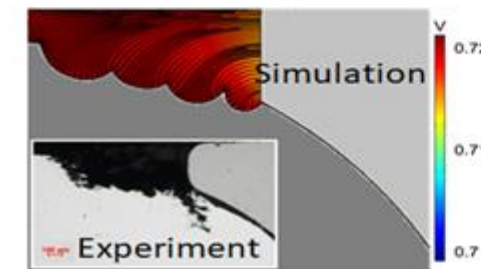
Corrosion with various nucleation input parameters are studied statistically.

- The distribution of the depth of corrosion is illustrated;
- The 95% confidence interval is [172.8, 251.4]. This is an indication of a more uniform corrosion growth.

Prediction of the corrosion nucleation and its evolution



SPR Prediction of corrosion after 26cycles

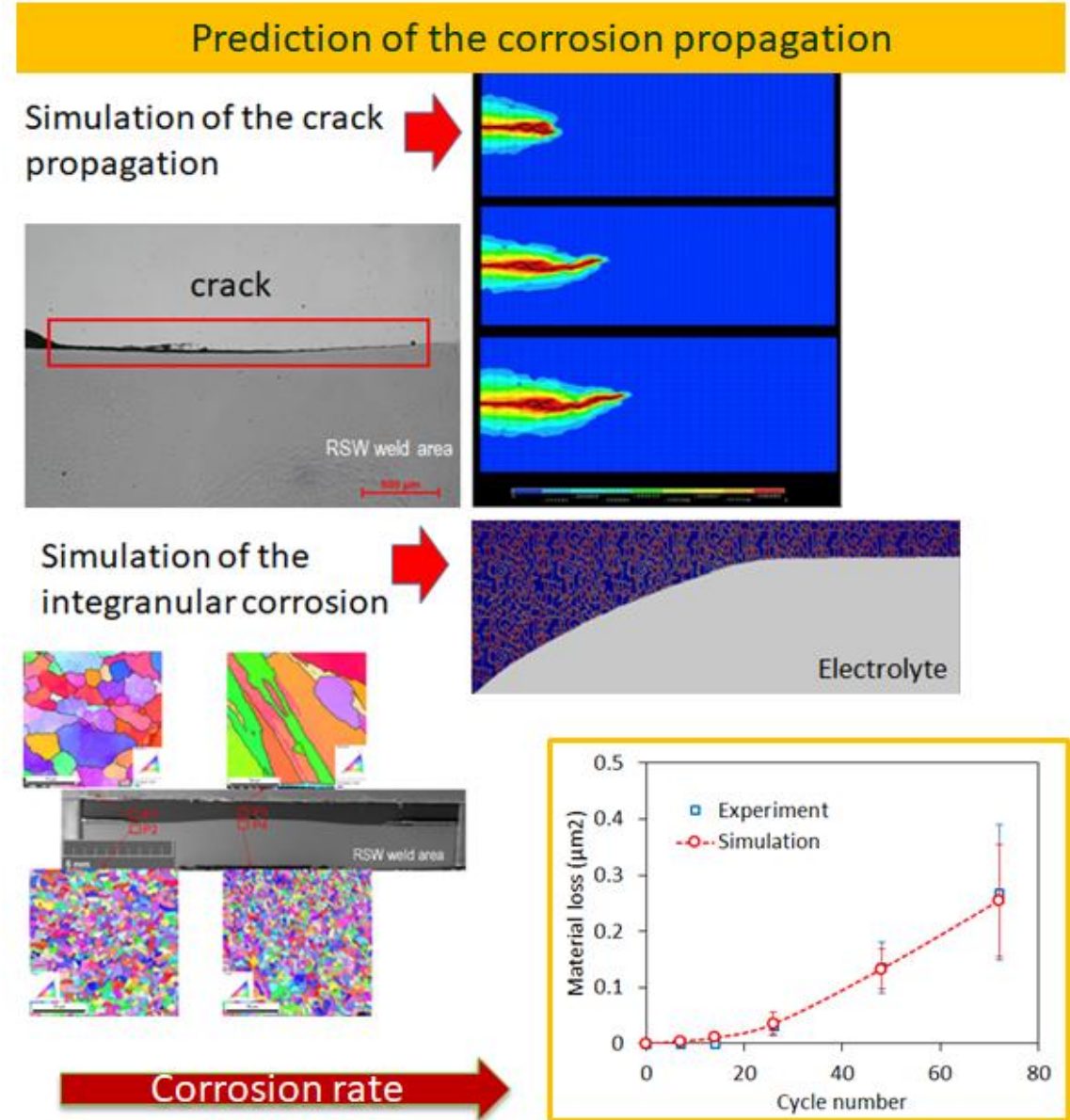


SPR Prediction of corrosion after 48cycles

Accomplishment

- The mesoscopic modeling accuracy for corrosion initiation and evolution was improved by modeling stress corrosion cracks (SCC) which were observed in experiments.
- SCC modeling combines the slip dissolution model with:
 - A modified phase-field model
 - Decohesion model based on hydrogen embrittlement mechanism
 - Peridynamics model
- **Dissolution of metal** (electrochemical sub-model) and **crack propagation** (mechanical sub-model) are coupled and simulated via phase field approach.
- Finite element model is combined with data driven models (PCA and SVM – Python library RiskPy available), deep learning and Sysweld – a commercial software for simulation of welding.

Corrosion rate was predicted with 5% error compared with the experiments for RSW and SPR using only axial cross sections of the joints.

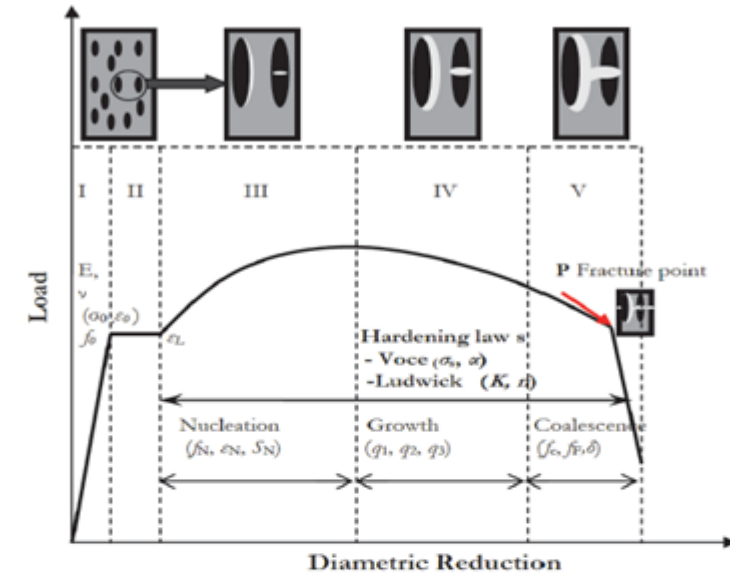


Accomplishment

- Lap shear finite element model includes selection of a constitutive material model for Al and steel coupons, welding interface and a corresponding damage model.
- As predicted at the atomic level scale and confirmed by lap-shear curves for corroded coupons, the mechanical behavior of the weld nugget is elasto-plastic up to 26 cycles of corrosion and become brittle after 48 cycles.
- To select a constitutive material model for the welding interface which models elasto-plastic and brittle behavior, a hypothesis was done “the material loss caused by corrosion generates a behavior similar with a ductile material with nucleation, growth and coalescence of the spherical voids”.
- Gurson–Tvergaard–Needleman (GTN) constitutive material model is selected to describe the influence of voids on plasticity properties of the metal.

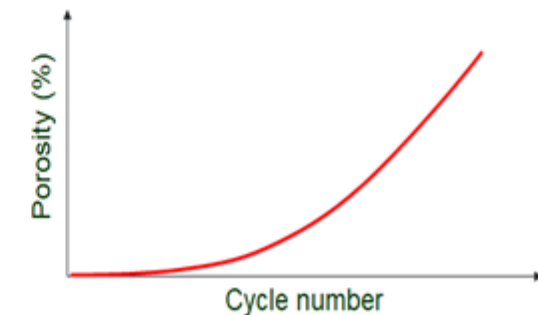
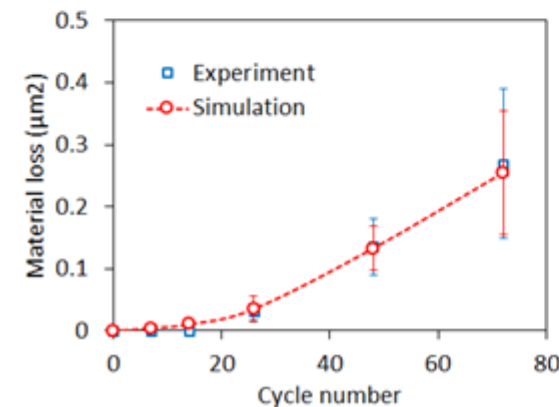
GTN constitutive model considered into the finite element simulation of the lap shear tests.

Description of the GTN model



M. Hadj Miloud et al., "Frattura ed Integrità Strutturale, 49 (2019) 630-642

Corrosion rate (mass loss or porosity vs. cycle number)

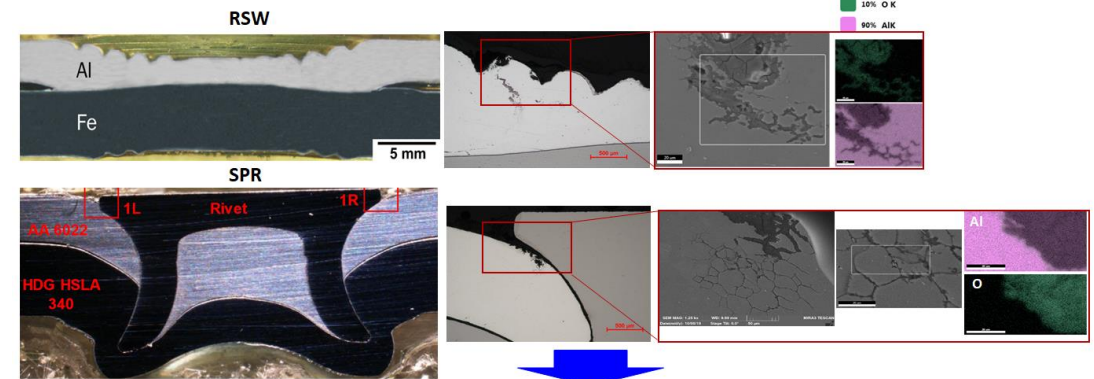


Accomplishment

- In GTN model, the corrosion mass loss ratio equals to the total effective void volume fraction (f^*) identified based on the corrosion rate or mass loss rate (predicted at the mesoscopic scale).
- To simulate nucleation, growth and coalescence, further identification of the GTN model parameters will be done based on mesoscopic level prediction and response surface method (RSM).
- The elastic properties of the weld nugget are calculated based on superposition law applied to the IMCs. The elastic properties of IMC were predicted and included in the material property database. Volume fraction of the IMCs is predicted at the atomic level scale and validated through microscopic imaging.

GTN constitutive material model is suitable for being used in simulation of the material loss from corrosion.

Mass loss through intergranular corrosion mechanism



Constitutive material model: Elastoplastic material which progressive change the behavior from ductile to brittle

Damage model: porosity based damage in ductile materials

- It is proposed a modified **Gurson–Tvergaard–Needleman (GTN)** model to for finite element simulation of the joint performance;
- Considering nucleation and growth of micro void in material.

$$\text{Yield surface in GTN model: } \Phi(\sigma_{eq}, \bar{\sigma}, f) = \frac{\sigma_{eq}^2}{\bar{\sigma}^2} + 2q_1 f^* \cosh\left(\frac{3}{2} q_2 \frac{\sigma_m}{\bar{\sigma}}\right) - (1 + q_1^2 f^{*2}) = 0$$

$$f^*(f) = \begin{cases} f & \text{if } f \leq f_c \\ f_c + \delta(f - f_c) & \text{if } f_c \leq f \leq f_F \\ f_U^* & \text{if } f \geq f_F \end{cases} \quad \delta = \frac{f_U^* - f_c}{f_F - f_c} \quad f_U^* = \frac{1}{q_1} \text{ when } q_3 = q_1^2$$

Φ : Yield Function, σ_{eq} : von Mises stress, $\bar{\sigma}$: equivalent tensile flow stress, σ_m : hydrostatic stress
 f^* : total effective void volume fraction, f : porosity, f_F : final fracture porosity, f_c : critical porosity,
 q_1, q_2, q_3 : void interaction parameters, f_U^* : ultimate porosity

Prediction of the joint performance in the following conditions:

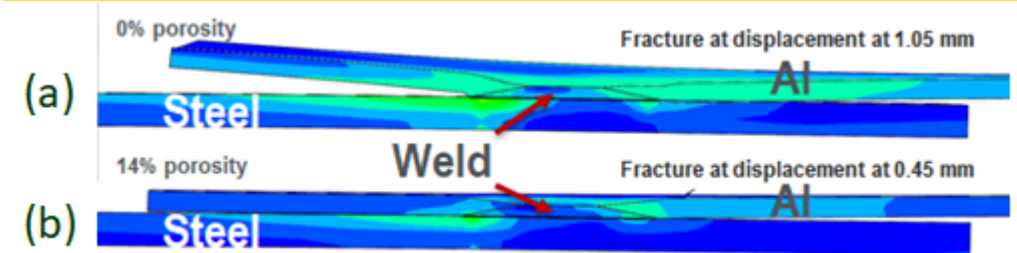
- 1.No corrosion (0 corrosion cycles)
- 2.Corrosion initiation (1-26 corrosion cycles corresponding to nucleation phase in GTN model)
- 3.Corrosion evolution (26-48 corrosion cycles corresponding to growth phase in GTN model)
4. Complete damage of the joint (72-104 corrosion cycles corresponding to coalescence phase in GTN model)

Accomplishment

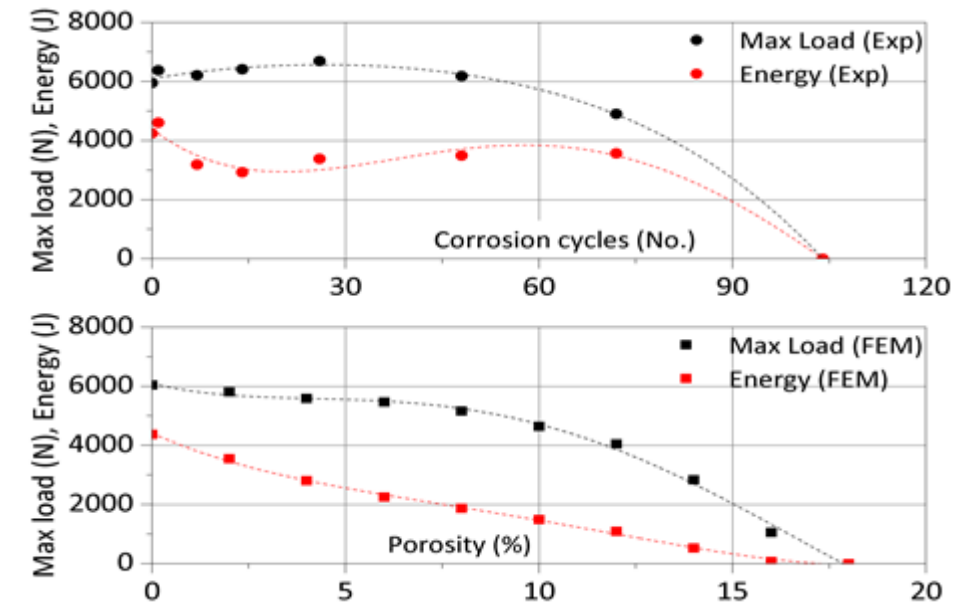
- In the first phase, a sensitivity study of the influence of void volume fraction (f^*) on prediction of the maximum load in lap shear tests for RSW joints was done.
- Preliminary tests were done in ABAQUS using the GTN model using $f^* = 0\%, 2\%, 4\%, 6\%, 8\%, 10\%, 12\%, 14\%, 16\%$. LS-Dyna tests are in progress.
- The sensitivity study confirms that at increasing in (f^*) produces a drop in the ductility of material and an early failure.
- Further mapping of the cycle number into the 3D material loss or porosity is needed for an accurate prediction of the f^* . However, in the first phase, when a random value of the porosity was chosen, the prediction error of the maximum load is around 10% comparing with the experiments. For no corrosion joints, the prediction error is 1% (porosity 0%).

Further tuning of its parameters based on 3D reconstruction of the porosity surrounding the weld nugget (RSW) and rivet (SPR) and homogenized mechanical properties of the corrosion products are needed to accurately predict the joining maximum load. [\(The deliverable is planned for September 2020\).](#)

Simulation of the lap-shear test using GTN model: (a) post welding before corrosion (0% porosity) and (b) after corrosion using an estimated porosity of 14%.



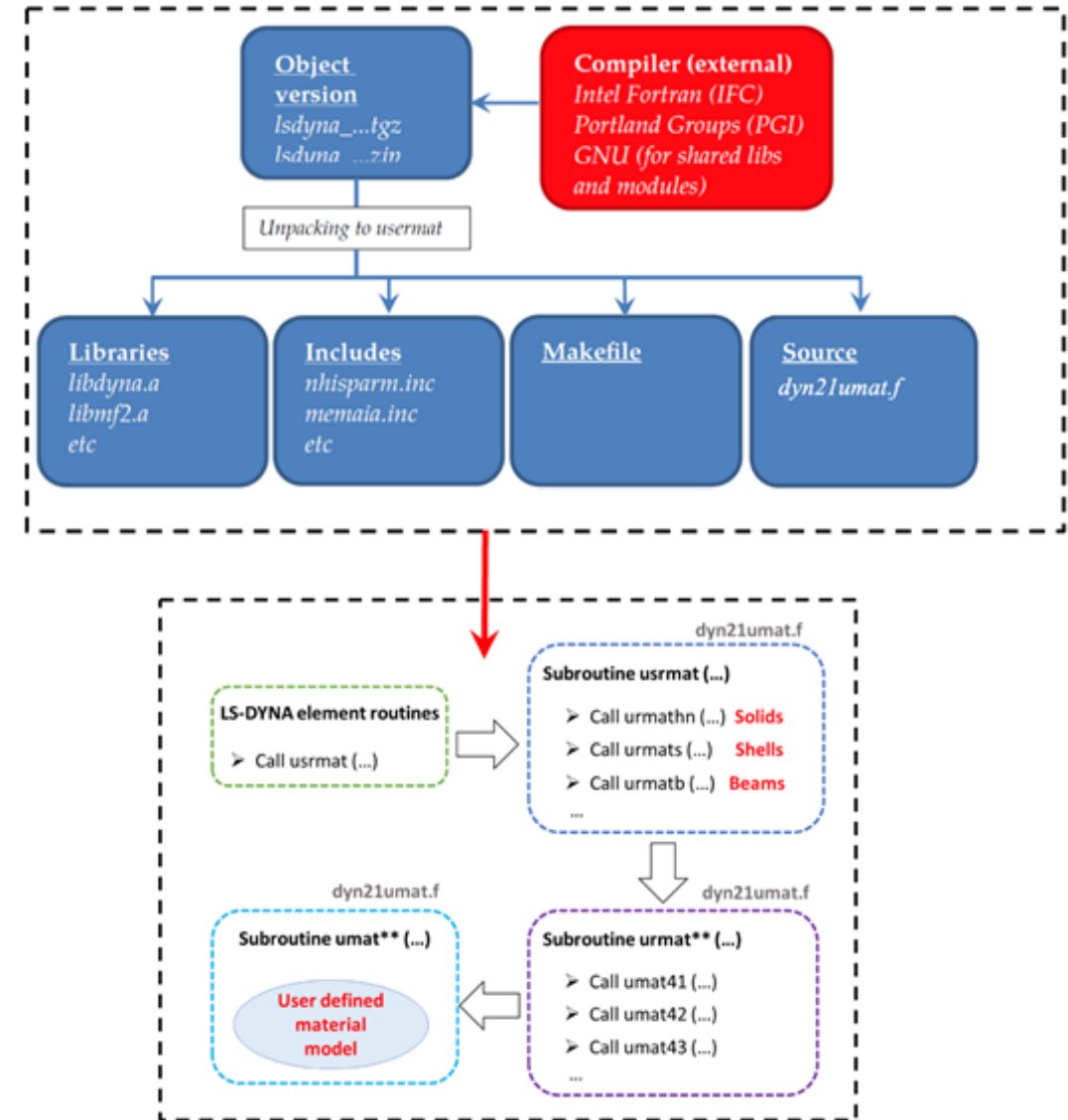
Prediction of the maximum load and energy dissipation for RSW joints with different porosities (corresponding to different corrosion levels). Comparison with the experimental values.



Accomplishment

- Defined material properties based on experimental and theoretical results. Identified a constitutive material model for corroded Al-Steel joints in LS-Dyna (GTN model).
- Established correlation between the material's elastic and plastic properties and the level of corrosion (corrosion rates predicted by the mesoscopic level model and the evolution of the mechanical properties of the corroded material - material loss).
- Developed material cards in LS-Dyna for describing the constitutive material model of the joints losing material through corrosion.
- Subroutines template were created for further input of the material properties considering corrosion.

The newly developed material cards (RSW and SPR) will include the mechanical properties of the metallic interfaces, parameters which are correlated with the corrosion rate depending on the pH suitable to be used with GTN model (LS-Dyna and Abaqus) or cohesive layer model. (The deliverable is planned for December 2021).



Responses to Previous Year Reviewers' Comments

The project was reviewed at the AMR. Two main concerns were:

Comment #1: The reviewer stated that only 12% of the project has been executed, so it is still early in the work. The reviewer provided a few things to consider and noted the following: very little was said about the corrosion test results in general; and it appears that some corrosion initiation sites were identified from the GM tests. The reviewer asked if the GM test results were from the testing done on specimens prepared as part of this program, or on specimens from another program. Very little was said about how the weld parameters for the three welding techniques under consideration were optimized. The reviewer asked what the final optimized welding conditions were. Very little said about the quality of welds obtained from the welds made.

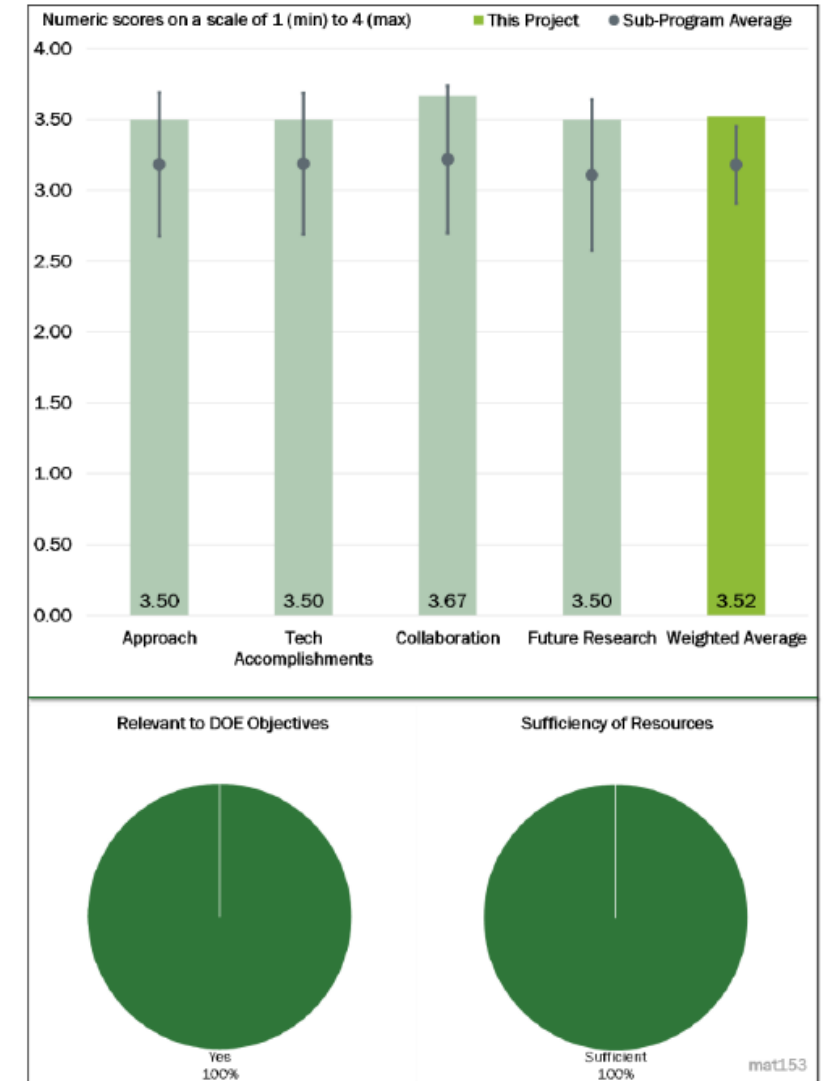
Response #1: The 2019 presentation at the AMR, the team shown an example based on preliminary tests done by GM on similar materials but not being included in the experimental plan of this project (project start date January 2019). Since then we completed all the number of joints using RSW, SPR and R-W. The parameters used for these processes are presented in Table 1 and Table 2. GM's and Henrob's extensive experience in RSW and SPR was used for setting up the process parameters so that a maximum possible strength of the joint to be obtained (lap shear test). R-W is a new technology developed by OPT. For this technology trial-and-errors were used for optimization the technology.

TABLE 1. WELDING PARAMETERS USED IN THIS STUDY (RSW)

Welding Force	900lb
Squeeze Time	250ms
Pre-heat Stage	40ms @7KA, 10ms cool
Welding Stage 1	250ms @12KA, 250ms cool
Welding Stage 2	975ms @13.4KA
Hold Time	250ms

TABLE 2. RIVETING PARAMETERS USED IN THIS STUDY

Rivet	Nominal diameter: 5 mm; Under-head shank length: 5mm; Type: countersunk; Material: Carbon steel and coated with zinc
Velocity	315 mm/s



2019 Annual Merit Review Report, mat_153 project evaluation

Responses to Previous Year Reviewers' Comments

The project was reviewed at the AMR. Two main concerns were:

Comment #2: The reviewer commented that future work focuses on modeling and simulation. However, not enough information is given to determine whether the future research will address the corrosion issues at hand. The reviewer cited as examples what parameter and features in the welds and coupons will be focused on to enable prediction of corrosion initiation from the modeling exercise, will these conditions and/or features be determined at the welding stage (weld parameters) or at the post-welding stage (after the welds have been formed), what role, for instance, will things like the kinetics of intermetallic formation play in corrosion initiation, and will volume fraction and distribution of intermetallic compounds plays a role as (of possibly many) in the modeling exercise. The reviewer advised please be specific as to what the authors are going to do in each of the three modeling and simulation exercises identified in your future work.

Response #2: The conditions for the corrosion initiation are determined post-welding stage. The factors which initiate corrosion in a car exposed to environmental conditions in winter and summer are: low/high temperatures, humidity and salt (pH). Similar conditions are created in the cyclic corrosion chamber where all the joints were exposed in an accelerated corrosion test (Slide 6). With an increased number of corrosion cycles, the corrosion is initiated and propagated intergranular producing mass loss (Slide 13).

The atomic level model predicts:

- (1) the IMCs phases which are formed in the welding and process (validated experimentally as shown in Slide 7);
- (2) The corrosion products by using thermodynamic and kinetic principles to tailor corrosion and its evolution illustrated by transformation of the IMC phases in other phases. This prediction is very important for the mechanical properties of the material which degrades with the corrosion evolution. When corrosion is installed the IMC phases which are ductile are transformed in corrosion phases which are brittle. Thus, the mechanical properties which will be input in finite element models has to take into account these values and their evolution associated with the corrosion rates.

Collaboration and Coordination with Other Institutions

University of Michigan (UM) – characterization of joining and modeling the performance prediction.

Penn State University (PSU) –mechanical behavior and interfacial phenomena, computational thermodynamics and kinetics.

University of Illinois (Illinois) –uncertainty quantification in multiscale modeling and building performance models.

Livermore Software Technology Corp (Ansys-LSTC) – developing a new material card for modeling corrosion.

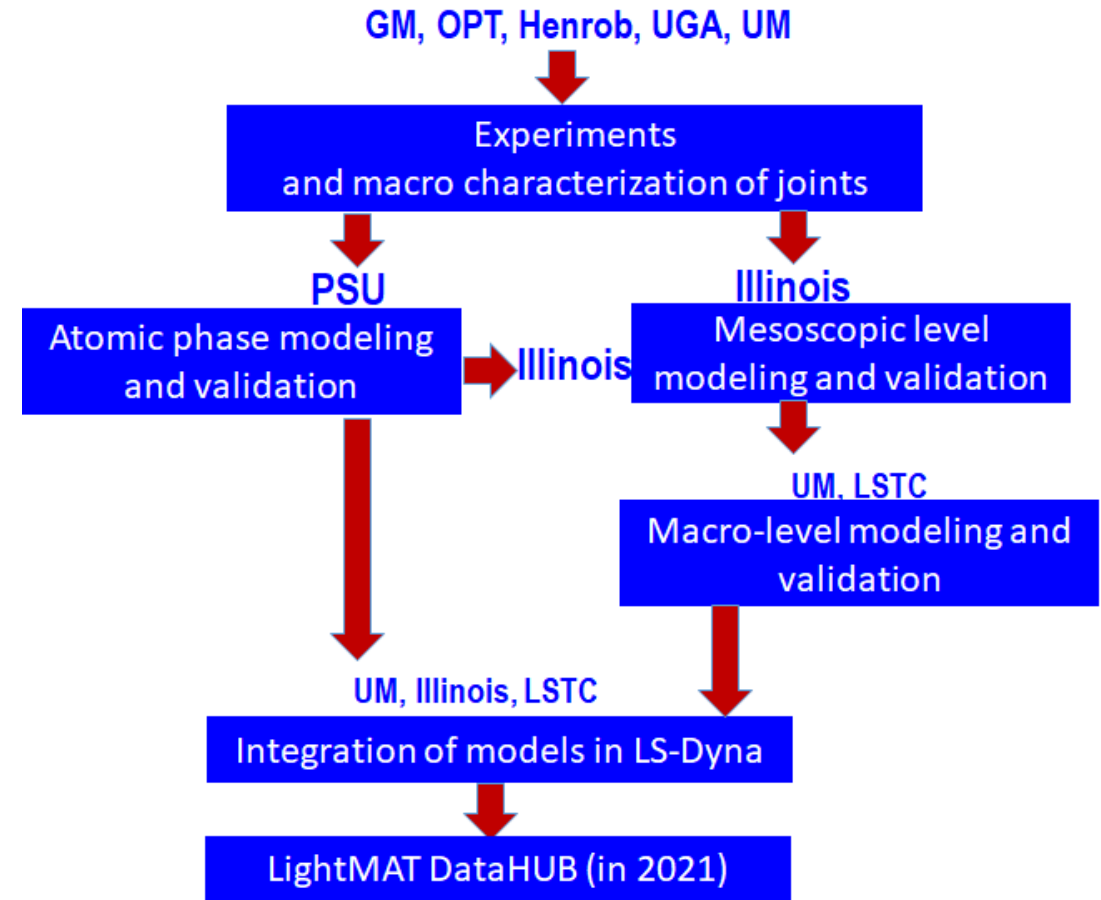
General Motors (GM)- provide facility for validation and demonstration of the RSW and SPR joints (together with Henrob).

Optimal Process Technologies, LLC (OPT) - provide facility for validation and demonstration of the Rivet-Weld technology.

University of Georgia – advise on design of R-W joint design and fabrication, analyze weld performance and its variation.

The team developed a collaboration flow which enable optimally use of the resources and equipment. In the first budgetary year it was demonstrated that this flow is efficient and productive.

Collaboration, Coordination and Sharing Facilities and Resources within the team

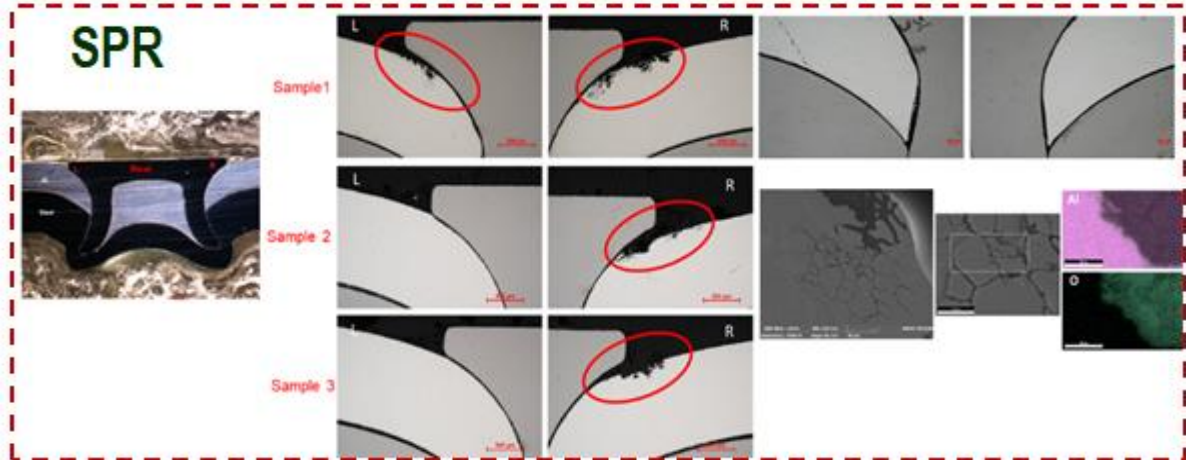
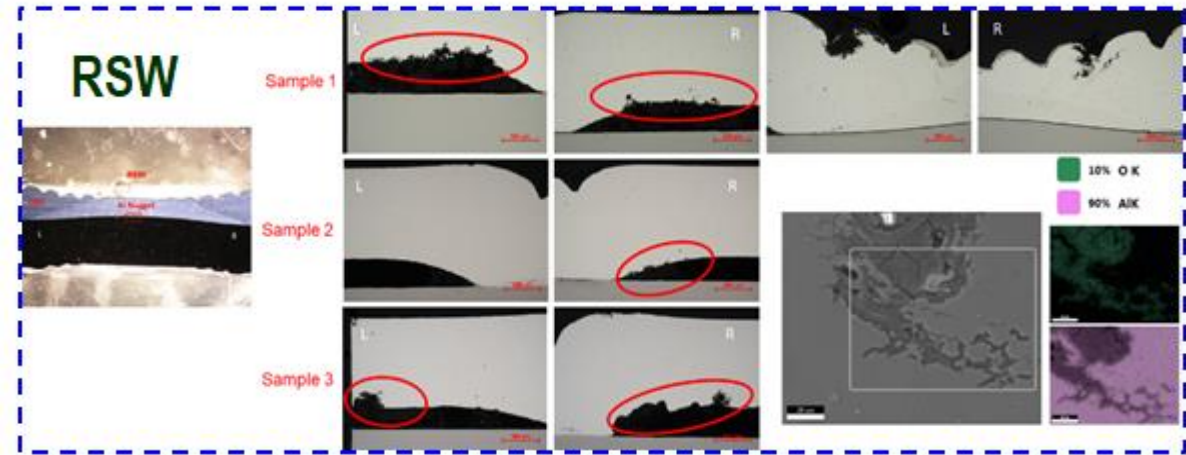


Remaining Challenges and Barriers

- Modeling non-uniform corrosion sites on the circumference of the welds observed in experiments. The team has two hypotheses: precisions of the electrode or rivet positioning with respect to the sheets which lead to small differences in the induced strain and consequently slightly different grain size on the circumference. Since corrosion mechanism is inter-granular it can impact the prediction. Coupons are hanged at 30° during the accelerated corrosion tests. Thus, one part will see a higher quantity of electrolyte and corrode faster.
- A sensitivity study is undergoing to track the position of the coupon in the chamber and correlation with further microscopic results in multiple cross sections surrounding the weld area. Grain size and their distribution are analyzed through EBSD analysis to quantify the differences along the circumference of the weld.

If the influence of the two factors is proved, it will certainly be considered in the mesoscopic model because the model counts galvanic corrosion (quantity of electrolyte) and intergranular corrosion. Thus, the model will be able to predict uncertainty in production.

RSW and SPR corrosion after 48 cycles. A cross section through the coupons indicating corrosion in left and right side with respect to the viewer.



Proposed Future Research

- Identification of the GTN model parameters for simulation nucleation, growth and coalescence. The identification will bridge the atomic level, mesoscopic level to macroscopic levels.
- Integration of the multi-scale models by correlation of the input parameters in the joining performance finite element model with the values from atomic scale and mesoscopic level. For example: the evolution of the mechanical properties of the corrosion products (atomic level modeling) will be homogenized for the vicinity of the welding area and rivet using mesoscopic models. The resulted set of Young's modulus and Poisson's ratio as well as their evolution during corrosion will be considered as input in the constitutive material model of the welding.
- The mesoscopic model which consider uncertainty quantifications will predict the corrosion rates in multiple planes surrounding the welding area (rivet area). Thus, the 3D joining performance model will be able to simulate non-uniform corrosion fronts observed from experiments due to variance of the welding conditions.
- Comparing the predicted force-displacement curves with lap shear experiments before and after corrosion.
- Finally, the force-displacement curves for RSW, SPR and R-W will be predicted and validated experimentally with an error <10%.

"Any proposed future work is subject to change based on funding levels"

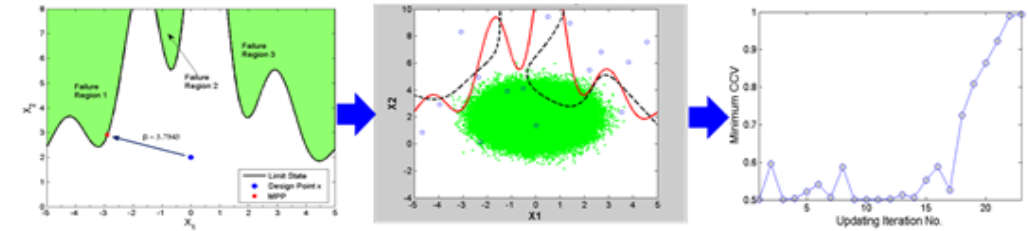
Proposed Future Research

- Corrosion evolution model verification and integration of the uncertainty quantification modeling. It will allow prediction of random events such as errors in positioning the RSW electrodes/and SPR, R-W rivet, variation of the equipment temperature due to mass production of the joining.
- Integrating a novel probabilistic confidence-based adaptive sampling (PCAS) technique into the multi-scale simulation platform.
- Fatigue performance prediction (S-N curves) for RSW, SPR, and R-W Joints by integrating traction stress method for demonstration of fatigue life predictability and an associated fracture mechanics criterion. This algorithm will be implemented as a nodal force based post-processing module to LS-Dyna and Abaqus.
- Validation of the predicted fatigue performance will be done based on experimental results of fatigue tests on coupons subjected to ambient and corrosion conditions.

"Any proposed future work is subject to change based on funding levels"

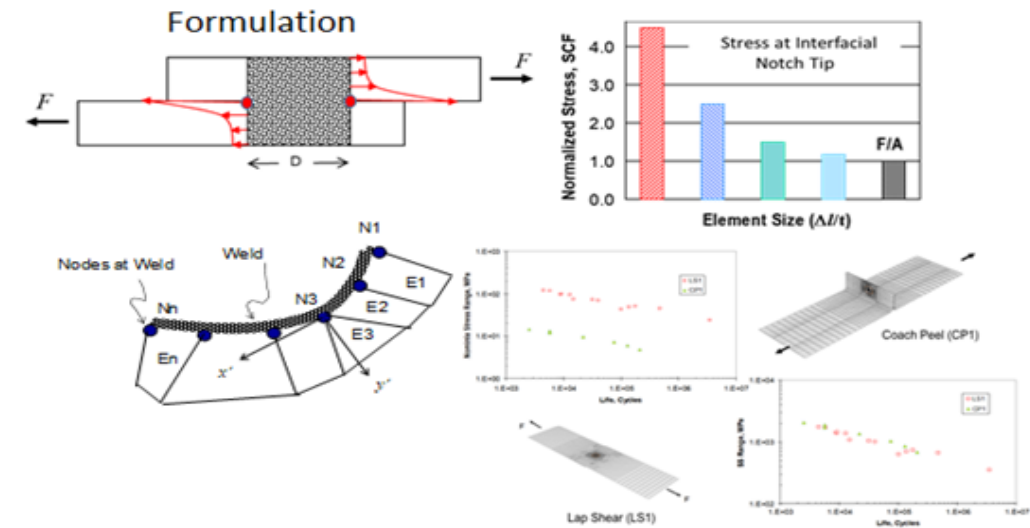
The PCAS technique

The PCAS Preliminary Results: an analytical testing problem



Approach	Probability Estimates	Error%	Total Num. of Simulations
MCS	2.56×10^{-4}	N/A	10^6
FORM	7.4×10^{-5}	71.09%	252
Gaussian Process	2.37×10^{-4}	7.42%	150
PCAS	2.55×10^{-4}	0.39%	38

Prediction of S-N curves



Effectiveness in S-N Test Data Correlation

Summary

- Microscopic atomic modeling from DFT-based first-principles calculations and phase-scale modeling from CALPHAD approach were developed to predict welding and corrosion products and their mechanical properties (5% error prediction comparing with experiments). A material database with the property parameters of the IMC compounds and corrosion products was established.
- Mesoscopic corrosion models were developed based on the finite element method and improved by incorporating SCC modeling and data-driven methods.
- Defined modeling standards for RSW performance joint simulation. Established the framework for the platform module for joint performance simulations in LS-Dyna.
- Initiated the simulation of joining performance and identified the constitutive material and model which is able to model corrosion and be able to connect with parameters identified at atomic level and mesoscopic scale.
- The resources and facilities were used in an optimized way so that all the milestones are on track.